HHS Public Access

Author manuscript

ACS Chem Biol. Author manuscript; available in PMC 2018 March 17.

Published in final edited form as:

ACS Chem Biol. 2017 March 17; 12(3): 643–647. doi:10.1021/acschembio.7b00031.

Substrate Trapping in the Siderophore Tailoring Enzyme PvdQ

Kenneth D. Clevenger[‡,⊥], **Romila Mascarenhas**[||], **Daniel Catlin**[||], **Rui Wu**[||], **Neil L. Kelleher**[⊥], **Eric J. Drake**[#], **Andrew M. Gulick**[#], **Dali Liu**[||,*], and **Walter Fast**[†,§,*]

[†]Division of Chemical Biology and Medicinal Chemistry, College of Pharmacy, The University of Texas, Austin, Texas 78712, United States

[‡]Biochemistry Graduate Program, The University of Texas, Austin, Texas 78712, United States

[§]Center for Infectious Disease, The University of Texas, Austin, Texas 78712, United States

[||]Department of Chemistry and Biochemistry, Loyola University Chicago, Chicago, Illinois 60660, United States

[⊥]Department of Chemistry, Northwestern University, Evanston, Illinois 60208, United States

[#]Hauptman-Woodward Medical Research Institute and Department of Structural Biology, SUNY University at Buffalo, Buffalo, New York 14203, United States

Abstract

Siderophore biosynthesis by *Pseudomonas aeruginosa* enhances virulence and represents an attractive drug target. PvdQ functions in the type-1 pyoverdine biosynthetic pathway by removing a myristoyl anchor from a pyoverdine precursor, allowing eventual release from the periplasm. A circularly permuted version of PvdQ bypasses the self-processing step of this Ntn-hydrolase and retains the activity, selectivity, and structure of wild-type PvdQ, as revealed by a 1.8 Å resolution X-ray crystal structure. A 2.55 Å resolution structure of the inactive S1A/N269D-cpPvdQ mutant in complex with the pyoverdine precursor PVDIq reveals a specific binding pocket for the D-Tyr of this modified peptide substrate. To our knowledge, this structure is the first of a pyoverdine precursor peptide bound to a biosynthetic enzyme. Details of the observed binding interactions have implications for control of pyoverdine biosynthesis and inform future drug design efforts.

Graphical Abstract

[*]Corresponding Authors: dliu@luc.edu. walt.fast@austin.utexas.edu.

Accession Codes

Coordinates and structure factors have been submitted to the Protein Data Bank as entries 5UBL for cpPvdQ and 5UBK for the PVDIq:S1A/N269D-cpPvdQ complex.

ORCID

Neil L. Kelleher: 0000-0002-8815-3372

Walter Fast: 0000-0001-7567-2213

The authors declare no competing financial interest.

Supporting Information

The Supporting Information is available free of charge on the ACS Publications website at DOI: 10.1021/acschembio.7b00031.

Materials, methods, crystallographic data, and structural overlays (PDF)

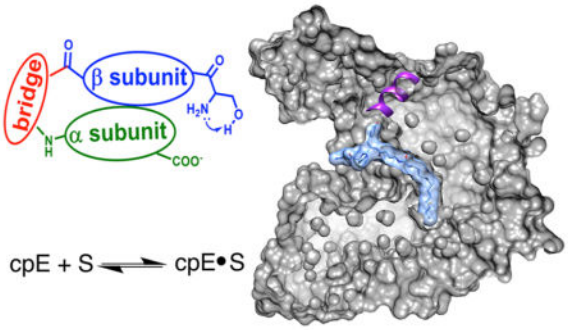

Current therapies for *Pseudomonas aeruginosa* infections are inadequate. More than 25% of deaths arising from all nosocomial Gram-negative infections are attributable to multidrug resistant *P. aeruginosa*.[1] Resistant strains employ multiple strategies to infect and thrive in host tissues, including production of siderophores.[2] To inhibit bacterial iron uptake, several lines of evidence point to the siderophore biosynthetic enzyme PvdQ as an attractive drug target. Pyoverdine (PVDI) has been shown to be the dominant iron uptake system in a mouse infection model,[3] and PvdQ catalyzes removal of the myristoyl anchor of the PVDI precursor PVDIq (Figure 1a).[4] Genetic disruptions of *pvdQ* result in *P. aeruginosa* strains that accumulate the myristoylated precursor PVDIq, fail to produce PVDI, are growth inhibited in iron-limited medium, are impaired in swarming and biofilm formation, and have drastically reduced virulence in plant and animal models of infection.[5,6] However, details of substrate:PvdQ interactions helpful for inhibitor development are lacking.

PvdQ is an N-terminal nucleophile (Ntn) hydrolase expressed as an inactive proprotein that undergoes self-catalyzed proteolysis to mature into an active heterodimer (Figure 1b).[7] The newly formed N-terminal amine of the β-subunit serves as a general acid and base during catalysis, highlighting one reason that the uncleaved proprotein is inactive.[8,9] Previous crystal-soaking and cocrystallization led to ligand:PvdQ structures that reveal a deep hydrophobic cavity selective for fatty acid chains 14 carbons in length, and a neighboring hydrophilic cleft open to solvent where, presumably, the peptide portion of PVDIq fits.[8,10,11] Almost all prior ligand:PvdQ structures show ligands that bind deep within the hydrophobic cavity and not at the hydrophilic site. Although the hydrophobic cavity provides opportunities for potent binding, there are limited possibilities for hydrogen bonding within this site to improve inhibitor selectivity. Details about the interaction of PvdQ with the peptidyl portion of PVDIq are absent. Herein we directly address this deficit by reporting the first structure of a substrate:PvdQ mutant complex.

Prior ligand:PvdQ structures were typically determined by characterizing noncovalent complexes with fatty acid products or by using low pH to trap a covalent ester intermediate, and do not reveal any information about interactions between PvdQ and the peptide portion of PVDIq. Preparing an inactive PvdQ mutant to trap the substrate is not straightforward since most of the residues essential for catalysis are also required for self-proteolysis during maturation (e.g., S217). For example, Ntn-hydrolases bearing mutations at the residue that becomes the catalytic N-terminus of the β-chain remain immature monomeric proproteins.[12]

Therefore, more extensive reengineering of the protein is required to disentangle the functions of residues in self-processing from their catalytic functions in substrate turnover.

To disconnect maturation from catalysis, we used a circular permutation[13] strategy to genetically reorganize the protein domains of PvdQ while retaining their structural orientation. Briefly, the *pvdQ* gene sequence was rearranged to first express the β-domain, followed by a -Gly-Ser-Ser- bridge, and ending with the original α-subunit (omitting the periplasmic sorting signal; Figures 1c, S1). Circular permutations have been reported for other Ntn-hydrolases.[14] For PvdQ, the bridging peptide was designed to provide a flexible and polar connection across the ~3.5 Å distance from the C-terminus of the β-subunit to the N-terminus of the α-subunit of wild-type PvdQ. Wild-type PvdQ is expressed as a proenzyme that purifies as a processed protein with α- and β-chains that effectively act as a heterodimer. However, expression and purification of the described circularly permuted PvdQ (cpPvdQ) resulted in a single polypeptide of approximately 80 kDa (Figure S2) containing rearranged α- and β-domains that correspond to the α- and β-subunits of wild type PvdQ.

Enzymatic activity of cpPvdQ was assessed using a series of *p*-nitrophenol esters of varying length[9] as alternative substrates, including esters of fatty acids 10, 12, 14, and 16 carbons in length (Table 1). Reordering the α and β domains of PvdQ by circular permutation only results in small perturbations of k_{cat} (1.1-fold increase), K_M (2-fold increase), and k_{cat}/K_M (1.7-fold decrease) values for the optimum substrate, *p*-nitrophenyl myristate. The selectivity profile was also quite similar between PvdQ and cpPvdQ, showing ≤4-fold differences between matched substrates across k_{cat}/K_M values ranging from 10^3 to 10^6 M^{-1} s^{-1}, indicating that the circular permutation had only minor effects on substrate selectivity.

The structural impact of circular permutation was assessed by X-ray crystallography. Despite domain reordering, cpPvdQ crystallizes in the same space group as PvdQ, $C222_1$.[9] A structural model of cpPvdQ was built and refined to 1.80 Å resolution and aligns very closely to wild-type PvdQ with an overall RMSD of 0.3 Å, including key amino acids reported to be involved in catalysis and substrate recognition such as S1 (*S217*), N269 (*N485*), V70 (*V286*), and F24 (*F240*) (Table S1, Figure S3). Residues are numbered based on the sequence of cpPvdQ, and the corresponding residue in wild-type PvdQ is referenced immediately thereafter in parentheses and italics for clarity. Electron density for the sequence linking β and α domains was observed, albeit weak for some residues and missing for the Ser residues in the (-Gly-Ser-Ser-) bridge (Figure S4). The newly installed bridge and the surrounding residues occupy a space in the crystal lattice that does not cause any major change among crystallographic contacts. Taken together, the functional and structural characterization of cpPvdQ indicates that the domain reordering only imparts subtle differences, making cpPvdQ a good model of PvdQ.

To trap unhydrolyzed substrate, mutations to inactivate cpPvdQ were introduced, and the resulting proteins assayed for hydrolysis of the *p*-nitrophenyl myristate substrate. The single mutant S1A-cpPvdQ, which lacks the side-chain of the catalytic nucleophile, has a 400-fold decrease in k_{cat}/K_M (3.5×10^3 $M^{-1}s^{-1}$). Although notably reduced, the activity is still significant, possibly due to solvent water substituting for the Ser1 side chain alcohol. A

different single mutant, N269D-cpPvdQ, was designed to place a negatively charged residue in the “oxyanion hole” used in the normal catalytic mechanism. The activity of N269D-cpPvdQ is less than S1A-cpPvdQ, but some substrate turnover was still detected after prolonged overnight incubations. Therefore, the double mutant S1A/N269D-cpPvdQ was prepared. This double mutant does not catalyze substrate hydrolysis greater than background levels.

A crystal of S1A/N269D-cpPvdQ was soaked with the substrate PVDIq, and a resulting structural model determined to 2.55 Å resolution (Figure 2, Table S1). At the active site, a simulated annealing omit map (Fo-Fc) reveals clearly formed electron density well fit by a portion of the unhydrolyzed substrate (Figure 2b). The observed density corresponds to the myristoyl substituent, the scissile amide bond linking this fatty acid to L-Glu and the isopeptide bond to the D-Tyr, and the L-Dab and D-Ser portions of the substrate, with the subsequent electron density becoming too diffuse to be accurately fit by the rest of the peptidyl portion of PVDIq. High resolution MS^1 and MS^2 spectra of the substrate confirm the presence of the cyclic peptide (Figure 3), so a lack of clear electron density indicates this portion of the substrate is not tightly bound in a single conformation. On the basis of the MS^2 spectrum, the structure of PVDIq matches a previous report that states the chromophore is not yet formed in this precursor,[15] consistent with our model in which the atoms that form the bond between L-Dab and D-Tyr rings in the chromophore are 4.3 Å apart.

Two additional aspects of the observed substrate:enzyme interactions are noted. First, the positions of S1A and N269D residues do not deviate significantly from the wild type. However, the carbon in the scissile amide bond of the substrate is repositioned by 1.2 Å, and this amide is rotated approximately 90° away from a reasonable attack angle, as gauged by comparison with the structure of wild type PvdQ in complex with a transition state analog inhibitor (Figure S5).[10] The bond rotation is possibly due to electrostatic repulsion between the substrate amide carbonyl oxygen and the N269D substitution. This bond rotation and the removal of the Ser1 side chain likely account for the loss of activity in this variant. Second, although the L-Glu, L-Dab, and D-Ser residues of the substrate do not appear to make specific interactions with the protein, the phenol group of D-Tyr does fit into a specific binding pocket, described below.

The phenol side chain of the substrate D-Tyr is bound to a PvdQ pocket through a number of specific interactions (Figure 2c). The phenol oxygen is within hydrogen-bonding distance of the backbone nitrogen atoms of both R297 (*R513*) and P296 (P512), as well as an ordered water molecule that is within hydrogen bonding distance of the backbone of A298 (*A514*), S268 (*S484*), and the side chain of D270 (*D486*). The D-Tyr ring is well positioned to make a cation–π interaction[16] with the side chain of R297 (*R513*). The hydrophobic portion of P296 (*P512*) and D269 (*D485*) as well as an edge-to-face π–π interaction[17] with the side chain of H457 (*H673*) surround the aromatic ring of D-Tyr. Finally, the phenol oxygen of D-Tyr points directly at the positive end of a putative helix dipole[18] from the α-helix comprised of residues P296–L305 (*P512–L521*), which terminates on the surface of the protein. These interactions clearly delineate a specific binding pocket within the hydrophilic cleft of PvdQ for the D-Tyr side chain of PVDIq.

In conclusion, circular permutation of an inactive PvdQ mutant enables trapping of unhydrolyzed substrate and reveals a specific binding pocket for the D-Tyr side chain of the pyoverdine precursor PVDIq. Structures of pyoverdine biosynthetic enzymes with amino acid precursors have been reported (*e.g.*, PvdA[19]), but to our knowledge, this is the first structure of a pyoverdine precursor peptide in complex with its biosynthetic enzyme. Elucidation of such bioprecursor:enzyme complexes offers an informative contrast with structures of completed siderophores. For one example, the structure of Fe^{3+}-bound pyoverdine in complex with the outer membrane receptor FpvA makes more extensive interactions with the cyclic peptide moiety.[20] In addition to providing guidance for inhibitor design efforts, the observed binding pocket for D-Tyr suggests that PvdQ is selective for siderophore precursors in which the chromophore has not yet been formed, placing PvdQ before PvdN, PvdO, and PvdP in the biosynthetic pathway,[4,21,22] and that PvdQ might select against exogenous acyl-siderophores lacking this D-Tyr.[23] Accommodation of L-Tyr at this position without major reorientation appears unlikely due to the short distance (5 Å) between the N269D β-carbon and the D-Tyr α carbon. Therefore, D-Tyr selectivity may serve as a quality control check for the upstream L-Tyr epimerase activity of PvdL.[24] In contrast, the lack of observed interactions between the cyclic peptide portion of the pyoverdine precursor and PvdQ indicates that this part of the substrate is not well recognized in the crystal and reveals how PvdQ might accommodate variations in pyoverdine peptide sequences that occur among *Pseudomonas* species.[25] Finally, although not discussed above, PvdQ has an alternative activity as a quorum-quenching enzyme.[8] The cpPvdQ variant developed herein provides a platform for developing variants to alter *N*-acyl-L-homoserine lactone processing in which mutations that effect activity and selectivity can be uncoupled from the maturation process.

METHODS

Detailed material lists and procedures are available in the Supporting Information.

Supplementary Material

Refer to Web version on PubMed Central for supplementary material.

Acknowledgments

Funding

This work was supported in part by National Science Foundation Grant CHE-1308672 (W.F. and D.L.), National Institutes of Health Grant AT009143 (N.L.K.), and the Robert A. Welch Foundation Grant F-1572 (W.F.).

For some of this work, we thank Argonne National Laboratory, Structural Biology Center at the Advanced Photon Source. Argonne is operated by UChicago Argonne, LLC, for the U.S. Department of Energy, Office of Biological and Environmental Research under contract DE-AC02-06CH11357.

References

1. Kaye KS, Pogue JM. Infections Caused by Resistant Gram-Negative Bacteria: Epidemiology and Management. Pharmacother. 2015; 35:949–962.
2. Lamb AL. Breaking a pathogen's iron will: Inhibiting siderophore production as an antimicrobial strategy. Biochim Biophys Acta, Proteins Proteomics. 2015; 1854:1054–1070.

3. Minandri F, Imperi F, Frangipani E, Bonchi C, Visaggio D, Facchini M, Pasquali P, Bragonzi A, Visca P. Role of Iron Uptake Systems in *Pseudomonas aeruginosa* Virulence and Airway Infection. Infect Immun. 2016; 84:2324–2335. [PubMed: 27271740]
4. Schalk IJ, Guillon L. Pyoverdine biosynthesis and secretion in *Pseudomonas aeruginosa*: implications for metal homeostasis. Environ Microbiol. 2013; 15:1661–1673. [PubMed: 23126435]
5. Nadal Jimenez P, Koch G, Papaioannou E, Wahjudi M, Krzeslak J, Coenye T, Cool RH, Quax WJ. Role of PvdQ in *Pseudomonas aeruginosa* virulence under iron-limiting conditions. Microbiology. 2010; 156:49–59. [PubMed: 19778968]
6. Papaioannou E, Wahjudi M, Nadal-Jimenez P, Koch G, Setroikromo R, Quax WJ. Quorum-quenching acylase reduces the virulence of *Pseudomonas aeruginosa* in a *Caenorhabditis elegans* infection model. Antimicrob Agents Chemother. 2009; 53:4891–4897. [PubMed: 19721066]
7. Huang JJ, Han JI, Zhang LH, Leadbetter JR. Utilization of acyl-homoserine lactone quorum signals for growth by a soil pseudomonad and *Pseudomonas aeruginosa* PAO1. Appl Environ Microbiol. 2003; 69:5941–5949. [PubMed: 14532048]
8. Bokhove M, Nadal Jimenez P, Quax WJ, Dijkstra BW. The quorum-quenching N-acyl homoserine lactone acylase PvdQ is an Ntn-hydrolase with an unusual substrate-binding pocket. Proc Natl Acad Sci U S A. 2010; 107:686–691. [PubMed: 20080736]
9. Clevenger KD, Wu R, Er JA, Liu D, Fast W. Rational design of a transition state analogue with picomolar affinity for *Pseudomonas aeruginosa* PvdQ, a siderophore biosynthetic enzyme. ACS Chem Biol. 2013; 8:2192–2200. [PubMed: 23883096]
10. Clevenger KD, Wu R, Liu D, Fast W. n-Alkylboronic acid inhibitors reveal determinants of ligand specificity in the quorum-quenching and siderophore biosynthetic enzyme PvdQ. Biochemistry. 2014; 53:6679–6686. [PubMed: 25290020]
11. Drake EJ, Gulick AM. Structural characterization and high-throughput screening of inhibitors of PvdQ, an NTN hydrolase involved in pyoverdine synthesis. ACS Chem Biol. 2011; 6:1277–1286. [PubMed: 21892836]
12. Bokhove M, Yoshida H, Hensgens CM, Metske van der Laan J, Sutherland JD, Dijkstra BW. Structures of an isopenicillin N converting Ntn-hydrolase reveal different catalytic roles for the active site residues of precursor and mature enzyme. Structure. 2010; 18:301–308. [PubMed: 20223213]
13. Yu Y, Lutz S. Circular permutation: a different way to engineer enzyme structure and function. Trends Biotechnol. 2011; 29:18–25. [PubMed: 21087800]
14. Li W, Cantor JR, Yogesha SD, Yang S, Chantranupong L, Liu JQ, Agnello G, Georgiou G, Stone EM, Zhang Y. Uncoupling intramolecular processing and substrate hydrolysis in the N-terminal nucleophile hydrolase hASRGL1 by circular permutation. ACS Chem Biol. 2012; 7:1840–1847. [PubMed: 22891768]
15. Hannauer M, Schafer M, Hoegy F, Gizzi P, Wehrung P, Mislin GL, Budzikiewicz H, Schalk IJ. Biosynthesis of the pyoverdine siderophore of *Pseudomonas aeruginosa* involves precursors with a myristic or a myristoleic acid chain. FEBS Lett. 2012; 586:96–101. [PubMed: 22172280]
16. Ma JC, Dougherty DA. The Cation-pi Interaction. Chem Rev. 1997; 97:1303–1324. [PubMed: 11851453]
17. Meyer EA, Castellano RK, Diederich F. Interactions with aromatic rings in chemical and biological recognition. Angew Chem, Int Ed. 2003; 42:1210–1250.
18. Sengupta D, Behera RN, Smith JC, Ullmann GM. The alpha helix dipole: screened out? Structure. 2005; 13:849–855. [PubMed: 15939016]
19. Olucha J, Meneely KM, Chilton AS, Lamb AL. Two structures of an N-hydroxylating flavoprotein mono-oxygenase: ornithine hydroxylase from *Pseudomonas aeruginosa*. J Biol Chem. 2011; 286:31789–31798. [PubMed: 21757711]
20. Greenwald J, Nader M, Celia H, Gruffaz C, Geoffroy V, Meyer JM, Schalk IJ, Pattus F. FpvA bound to non-cognate pyoverdines: molecular basis of siderophore recognition by an iron transporter. Mol Microbiol. 2009; 72:1246–1259. [PubMed: 19504741]
21. Ringel MT, Drager G, Bruser T. PvdN Enzyme Catalyzes a Periplasmic Pyoverdine Modification. J Biol Chem. 2016; 291:23929–23938. [PubMed: 27703013]

22. Nadal-Jimenez P, Koch G, Reis CR, Muntendam R, Raj H, Jeronimus-Stratingh CM, Cool RH, Quax WJ. PvdP is a tyrosinase that drives maturation of the pyoverdine chromophore in *Pseudomonas aeruginosa*. J Bacteriol. 2014; 196:2681–2690. [PubMed: 24816606]

23. Kem MP, Butler A. Acyl peptidic siderophores: structures, biosyntheses and post-assembly modifications. BioMetals. 2015; 28:445–459. [PubMed: 25677460]

24. Visca P, Imperi F, Lamont IL. Pyoverdine siderophores: from biogenesis to biosignificance. Trends Microbiol. 2007; 15:22–30. [PubMed: 17118662]

25. Cezard C, Farvacques N, Sonnet P. Chemistry and biology of pyoverdines, *Pseudomonas* primary siderophores. Curr Med Chem. 2015; 22:165–186. [PubMed: 25312210]

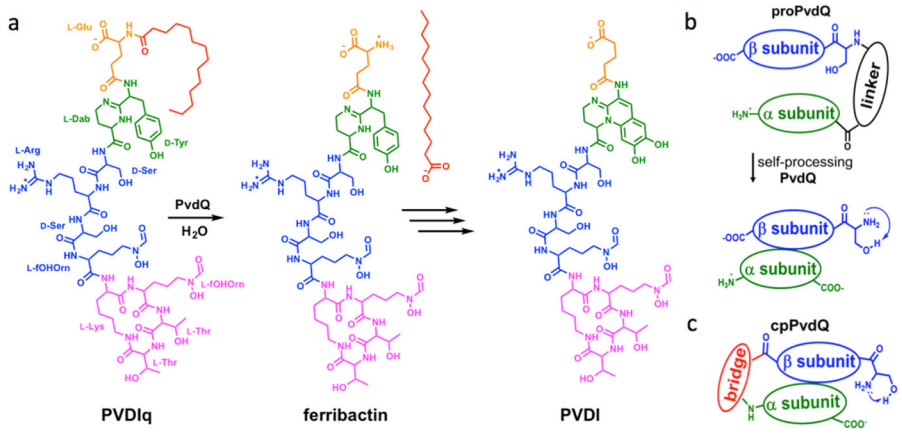

Figure 1.

PvdQ function, self-processing, and circular permutation. (A) Scheme shows PvdQ catalyzed hydrolysis to remove a myristoyl group from the biosynthetic precursor PVDIq to produce the ferribactin product that is eventually converted to pyoverdine (PVDI). The myristoyl group is shown in red, linker in orange, chromophore (precursors) in green, linear peptide portion in blue, and cyclic peptide portion in purple. (B) Self-proteolysis of the PvdQ proprotein leads to loss of a 23 residue linker peptide and formation of a heterodimer that relies on the newly formed β N-terminus to activate the catalytic nucleophile. (C) cpPvdQ has rearranged domains that circumvent the need for self-proteolysis.

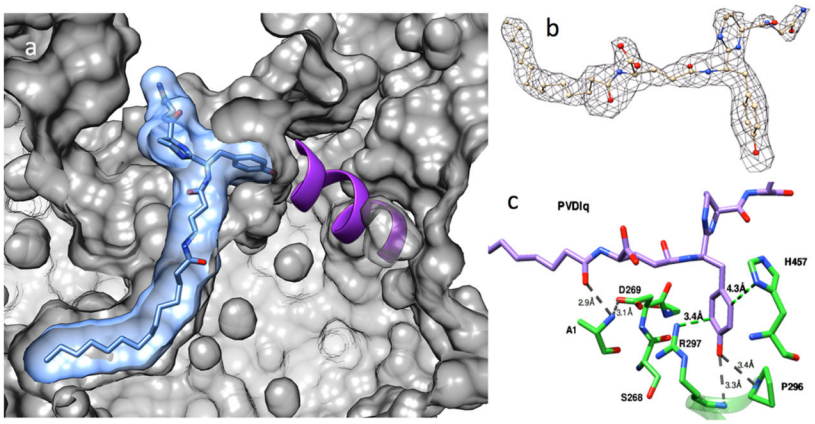

Figure 2.

X-ray crystal structure of PVDIq:S1A/N269D-cpPvdQ. (A) A cut-away view shown of S1A/N269D-cpPvdQ (gray) bound to PVDIq (blue) is shown with surfaces for each component, and the interacting P296–L301 α-helix (purple) shown as a ribbon. (B) A simulated annealing omit map (Fo-Fc) of bound PVDIq is shown with a density at 2.4 σ. A portion of unhydrolyzed PVDIq, shown as ball and stick, fits within the observed density. (C) Details of the binding pocket for the D-Tyr of PVDIq are shown. cpPvdQ (green) is shown with a portion of the P296–L301 α-helix as a ribbon. PVDIq (purple) is shown with H-bond distances in gray dotted lines and estimated cation–π and edge-to-face π–π interaction distances in green. Distances are subject to coordinate errors listed in Table S1.

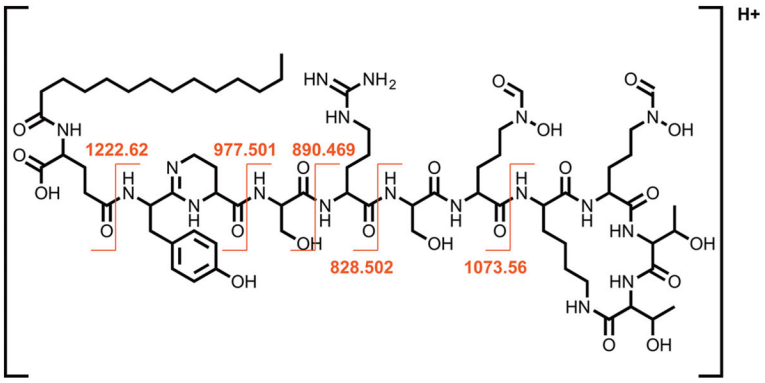

Figure 3.

PVDIq fragment ions confirming the structure of PVDIq. A map of b and y ions detected from PVDIq MS^2 fragmentation is shown. The molecular cation of PVDIq with m/z = 1561.858 was detected in MS^1 mode with a predicted molecular formula of $C_{70}H_{116}N_{18}O_{22}$ (1560.852 Da observed, 1560.851 Da theoretical, 0.2 ppm error). Diagnostic b and y ions characteristic of the expected fragmentation of PVDIq amide bonds in MS^2 mode confirmed the ligand's structure as that previously proposed for PVDIq (Figure 1).[15] All fragments ions are within 5 ppm of theoretical m/z values and match those previously reported for PVDIq.[15]

Table 1

Steady State Kinetic Parameters

enzyme variant	[S] size[a]	K_M (μM)	k_{cat} (min^{-1})	k_{cat}/K_M (M^{-1} s^{-1})
PvdQ[b]	10	60 ± 10	49 ± 5	1.3×10^4
PvdQ[b]	12	0.8 ± 0.1	52 ± 3	1.1×10^6
PvdQ[b]	14	0.60 ± 0.06	86 ± 3	2.4×10^6
PvdQ[b]	16	4 ± 1	1.9 ± 0.1	8×10^3
cpPvdQ	10	N.D.[c]	N.D.[c]	1.5×10^4[,d]
cpPvdQ	12	1.3 ± 0.2	38 ± 1	4.9×10^5
cpPvdQ	14	1.2 ± 0.2	98 ± 5	1.4×10^6
cpPvdQ	16	1.3 ± 0.2	2.5 ± 0.1	3.1×10^4

[a] The number of carbon atoms in the fatty acid moiety of *p*-nitrophenol ester substrates ([S]).

[b] Values for wild type PvdQ are taken from ref (9).

[c] Not determined because substrate K_M values were larger than the solubility limit of the substrate.

[d] Fitting error is <10%.